

Shrinkage alteration in the function of segregation of glass beads in injection molded

PA6

Kovács J. G.

Accepted for publication in Polymer Engineering and Science

Published in 2011

DOI: [10.1002/pen.22025](https://doi.org/10.1002/pen.22025)

TITLE:

**SHRINKAGE ALTERATION IN THE FUNCTION OF SEGREGATION OF GLASS BEADS IN INJECTION MOLDED PA6**

AUTHOR:

**J. G. KOVÁCS<sup>1</sup>**

<sup>1</sup>CORRESPONDING AUTHOR, DEPARTMENT OF POLYMER ENGINEERING, BUDAPEST UNIVERSITY OF TECHNOLOGY AND ECONOMICS, BUDAPEST, HUNGARY,  
TEL.: +36 (1) 463-14-40, FAX.: +36 (1) 436-15-27, KOVACS@PT.BME.HU

## **1. Abstract**

A new method is introduced to evaluate the segregation effect of glass beads in injection molded nylon parts. Mass measurement technique was used to measure inhomogeneous distributions of glass particles along the flow path during the injection molding process. Experiments were done on injection molded polyamide 6 (PA6) composites with solid glass bead (GB) contents of 10, 20, 30, 40 wt% and diameters of 11, 85, 156, 203  $\mu\text{m}$ . It was concluded that the flow-directional segregation depends on both the diameter and the concentration of the glass beads. In addition, segregation affects the distribution of volumetric shrinkage along the flow path, playing a major role in the dimensional accuracy of the part. In this paper a new model is introduced to extend shrinkage calculations to include the effect of glass beads and segregation.

## **2. Keywords**

particle size distribution; injection molding; fillers; polyamides

### 3. Introduction

The mechanical properties of injection-molded polymer composites are determined by their macro structure (geometry, concentration, distribution, orientation) and their micro structure (morphology, properties of the components and their impact on each other) [1]. During product design the engineer chooses the material – reinforced or filled – based on the future use of the product, assuming that the properties of the material at any point of the geometry are identical to its nominal values. The mechanical and other properties of the product (such as conductivity) are significantly influenced by the filler and reinforcing agent content as well as their parameters during various processing techniques. In order to achieve optimal mechanical properties for the piece (as well as homogeneous reinforcement and filler distribution), the features of the processing technology and the effect of the processing parameters should be taken into account.

It has been noted that the distribution of the solid particles is inhomogeneous in both transversal and longitudinal directions in the case of injection molded products containing fillers or reinforcements. This property is called segregation.

#### **The effect of filler or reinforcement shape on segregation**

Researchers dealing with the inhomogeneous distribution of fillers or reinforcements during injection molding studied the phenomenon in the case of various types ( $l/d$ ) of filler or reinforcements, diameter and concentration. Their experiments will be shown below ordered by type, size and concentration of them as well as by the establishment of the applied gate.

Hegler and Mennig [1, 3] studied segregation by producing glass fiber and glass bead filled thermoplastics (PA6 and SAN dumb-bell sample). They observed that in the

direction of flow the distribution of the filler and reinforcement is a function of its geometry, i.e. function of  $l/d$ . In the case of glass beads ( $\sim 156 \mu\text{m}$ , 45 wt%) where the value of  $l/d$  is small ( $\sim 1$ ) by the end of the flow the filler content exceeded its nominal value by  $\sim 4$  wt%. In contrast, using short glass fiber where the value of  $l/d$  is large, the reinforcement content did not differ from its nominal value.

Kamal and Singh [4] studied the morphological properties of injection molded specimens with polypropylene matrix containing 30 wt% short glass fibers. For their experiments they used a 100x60x3 mm specimen with a 7.8 mm wide semicircular cross-sectional gate on the shorter side. They observed that the fiber content deviation from the nominal value is no more than  $\pm 5$  wt% in the direction of the flow. Near the gate, the fiber content decreased whereas at the end of the flow higher density of fibers was observed. This effect in the cross-sectional area at the edge of the product was less significant than in the direction of the gate.

O'Regan and Akay [5] studied the variation in fiber length and content distributions (50 wt%) in the direction of the flow and the thickness. They used injection molded PA66 samples. They concluded that the fiber length was significantly influenced by the type of nozzle (open or needle-valve nozzle) and the gate type. In the direction of flow away from the gate, the fiber length decreased, while the fiber content increased (3-10 wt%). Based on their experiments, the fiber content did not change near the gate.

Lafranche et. al. [6] investigated fiber breakage and segregation along the flow axis as well as perpendicular to the flow direction in the case of PA66 long fiber thermoplastic injection moldings. They observed that the fiber content from the samples near the gate was less than the nominal 42 wt% ( $\sim 38.5$  wt%) and towards the end of the

flow it reached 51 wt%. The nonlinearity of the change in fiber content was not discussed.

#### **The effect of filler diameter on segregation**

By increasing the glass bead diameter (from ~25  $\mu\text{m}$  to ~156  $\mu\text{m}$ ) Hegler and Mennig [1, 3] observed that at the end of the flow the bead content increased from the nominal 45 wt% to 48 wt% for SAN and to 50 wt% for PA6.

Papathanasiou and Ogadhoh [7, 8] filled glass beads into PS matrix (bead diameters fell within ranges 40-75  $\mu\text{m}$ , 80-115  $\mu\text{m}$ , 160-250  $\mu\text{m}$ , 250-400  $\mu\text{m}$ , 425-500  $\mu\text{m}$ ). They observed that in the flow direction the effect of segregation is negligible in the case of small beads (40-75  $\mu\text{m}$ , 80-115  $\mu\text{m}$ ); in contrast, by increasing the bead size, the effect became more notable. They showed that the beads' distribution near the gate is significantly influenced by the gate type and location, whereas further from the gate this effect decreases then completely disappears.

#### **The effect of filler and reinforcing material content on segregation**

Hegler and Mennig [2, 3] studied the segregation of the filler using different glass bead content (15, 30, 45 wt%; ~156  $\mu\text{m}$ ) in the SAN and PA6 matrix systems. They observed that in the case of PA6 the increase in nominal filler content increased at the end of the flow by 0.5, 0.75 and 4.7 wt%. Using the SAN matrix the increase of the glass bead content at the end of the flow was ~3 wt%, independent of the nominal filler content. The authors did not discuss the change in segregation for the different matrices.

#### **The effect of gate arrangement on segregation**

Papathanasiou and Ogadhoh [7, 8] studied the bead distribution near the gate and along the flow axis using two different gate designs. They observed that for gates in flow direction, perpendicular to the flow (x-y plane) the bead concentration is minimal

near the gate, while for gates perpendicular to flow direction, this concentration can be made more uniform. In the direction of flow away from the gate – independent of gate arrangement – an increase in bead concentration was observed which was explained by the fountain flow.

### **The effect of product geometry on segregation**

After examining the cross-sections of samples, Hegler and Mennig [2, 3] found that segregation along the thickness – in the case of symmetrical mold cooling – is symmetric to the product midline. While studying PA66 systems filled with 50 wt% long or short fiber O'Regan and Akay [6] noticed that by increasing the temperature of the moving mold half by 15°C, the symmetric reinforcement distribution becomes asymmetric. In further research using tubular and spiral shaped sample parts, Hegler et al. [3] observed that part weight and increase in flow length enhances segregation. From their experiments on fiber content along the thickness Kamal and Singh [4] observed a fiber free zone along the wall that they explained by the shear-profile along the specimen's thickness: the particles moved towards the smaller shears.

Papathanasiou and Ogadhoh [7] observed inhomogeneous bead content along the specimen's thickness even in the case of the smallest glass bead diameter (40-75  $\mu\text{m}$ ) that they used. They explained this with a cumulative effect: the beads are located in the middle of the melt (at the least sheared layer) entering the nozzle. Entering the cavity and going further from the gate, this inhomogeneity disappears due to the fountain flow. The second effect is the beads' lateral movement from the strongly sheared layer towards the less sheared middle plane. By combining these two effects, it can be observed that in the bead distribution along the thickness – away from the gate

along the flow – the initial sparse-dense-sparse structure gradually becomes an average-sparse-dense-sparse-average structure.

Jana [9] studied the segregation of sphere-shaped conducting particles (Ketjenblack 600JD, Akzo Nobel, 1.5 wt%) along the thickness in PP matrix. He noticed that the conductivity of the composites was not in accordance with the nominal filler content. By milling the surface repeatedly, he showed that away from the specimen's wall towards the core layer the concentration of the conducting particles is increasing. Following Jana's [9] work, Hong et al. [10] studied the conductivity of composites made by particles filled into PP and PS matrices (Ketjenblack, Akzo Nobel). They observed that by increasing the injection speed, the specimen's conductivity decreased. By removing the surfaces by laser, they found that the thickness of the layer without many conducting particles near the surface is increasing by increasing the injection speed, i.e. by increasing the shear.

Hong and Jana [11] investigated segregation along the thickness of injection molded PP and PS systems filled with 42 and 203  $\mu\text{m}$  diameter solid glass beads (Potters) (15, 20 and 30 wt%) and they also compared the mechanical properties of these systems to those of similar pressed molded systems. Using SEM images of the fractures, they observed that while the distribution of glass beads is homogeneous in the cross-sectional area of press molded specimens, the bead concentration increases from the edge (no beads) towards the middle plane of injection molded specimens. They also noticed that the width of the region without the beads is larger when using smaller beads or when the injection speed is higher.

Lafranche et al. [6] determined that in their injection molded PA66 specimen filled with long glass fibers, the fiber distribution through the thickness is homogeneous

near the gate. This distribution becomes inhomogeneous along the flow axis: the fiber concentration increases near the mid-plane of the part. They explain this phenomenon with the breakage of fibers embedded into the shell layer as the shear flow breaks them.

Lafranche et al. [6, 12] found that the reinforcement content distribution is homogeneous near the gate along the thickness, while Papathanasiou and Ogadhoh [8, 9] noticed inhomogeneous filler content distribution along the thickness. This supposed discrepancy is due to different gate arrangements in the two experiments: Lafranche et al. used a 4 mm fan gate that is thicker than the specimen (3 mm), while Papathanasiou and Ogadhoh utilized a standard gate smaller than the specimen's thickness and width.

#### **The mathematical modeling and simulation of segregation and shrinkage**

During the 80's several researchers [13-24] report a movement perpendicular to the spherical filler residue flow for concentrated solutions, and they also study the mathematical modeling of this phenomenon. To describe this phenomenon in shear induced flow, Leighton and Acrivos [15, 16] propose a model describing the filler movement based on the irreversible interaction between particles. Using scale-factors they establish a dependency that describes the fluxus diffusion in the case of simple shear flow (e.g., so-called Couette-flow between the layers of a plane-plane rheometer) [16].

## **4. Materials and methods**

PA6 matrix filled with solid glass beads of different diameters (11, 85, 156, 203  $\mu\text{m}$ ) and contents (10, 20, 30, 40 wt%) were studied. The matrix (Lanxess, Durethan B30S) and the beads (Potters Industries Inc., Spheriglass® with coupling

agent) were mixed on a Brabender Plasticorder 814402 type twin-screw extruder with constant screw revolutions per minute. A Brabender pelletizer was used to produce pellets from the extrudate. The glass bead content of each material was verified by determining the ash content where the maximum deviation was 3.7 wt% from the nominal values.

From these materials 80x80x2 mm specimens were injection molded with a special mold (Fig.1.) on an Arburg 320C 600-250 injection molding machine at melt temperature 280°C, mold temperature 80°C and volumetric flow rate 50 cm<sup>3</sup>/s. Five measurement locations were marked (Fig.2.) on each specimen where the appropriate dimensions were measured at 1 hour after demolding using a Mitutoyo digital caliper, with two decimal digit precision. The linear shrinkages were determined from the measured dimensions of the specimens and the nominal dimensions of the cavity.

After each shrinkage measurement, the glass bead content was determined according the EN ISO 3451:1-1999 standard. After burning in the open air for 10 minutes, the remaining thermoplastic material was burned out at 450°C for 480 seconds in a Nabertherm oven. The remaining ash was measured with an Ohaus Explorer laboratory scale with 0.0001 g precision. The segregation was determined on the flat specimens by measuring the bead content at different positions. A preliminary experiment was done by measuring nine different positions (Fig.3.) to analyze both the flow and cross-flow induced segregation. In subsequent measurements to characterize segregation along the flow direction only, the samples were cut into either 5 or 14 strips (Fig.4.) with a Mutronic DiaDisc 4200 sample cutter. After the burning process, the diameters of the glass beads in each sample were determined with Malvern Mastersizer Particle Size Analyzer 2000.

## 5. Results and discussion

The effect of segregation was examined both along the flow direction and perpendicular to the flow direction during injection molding. The influence of the segregation effect on the shrinkage properties was also analyzed.

Segregation was initially measured at three different positions in the flow direction and three different positions perpendicular to the flow direction (Fig.3.). It was concluded that the content of the glass beads is uniform in the cross-flow direction, while the divergence of the beads are quite high in the flow direction (Fig.5.). This difference between the two directions occurs because the material fills up the cavity uniformly from the film gate. Based on this result, only the flow directional segregation was examined further.

In order to determine the optimal number of measured samples in the flow direction, samples from the initial experiment (Fig.3.) were compared to samples from two plates cut into 5 and 14 parallel strips, respectively (Fig.4.). The results are shown in Fig.6. Given the difficulties of the 14-sample preparation and since the measurements for the three resolutions showed no major differences in accuracy (Fig.6.), 5 samples were used for all subsequent measurements.

According to Hegler and Mennig [1] gravity could have an effect on the segregation. As the injection mold has two cavities next to each other in the vertical direction, the one on the bottom likely has an advantage during the filling stage because of the gravity effect. The influence of this gravity effect was tested in the case of 40 wt% glass beads filled material. Segregation measurements were similar in the two sides; only a minor effect was found, but the scatter of the measurement was higher than the effect itself.

Finally all 16 different materials were used for both the segregation measurements and the shrinkage measurements. On each sample, the segregations were measured at 5 different places (Fig.4.) and the shrinkages were measured at 2 different places, one near the gate and one near the end of the flow. Segregation is negligible in the case of the smallest glass beads (average diameter 11  $\mu\text{m}$ ) (Fig.7.).

With the smallest (11  $\mu\text{m}$ ) glass beads, segregation won't occur even when the content increases to 40 wt%. However, the rising particle size has an effect on segregation as the amount of the glass beads increases (Fig.8-10.).

The largest particles show considerable difference along the flow path. It can be seen that next to the gating area the content of the beads dropped to 34 wt% from the nominal 40 wt%, while at the end of the flow it increased above 48 wt% (Fig.10.).

The segregation effect is more significant as the amount of the glass beads increases. While low amount of glass beads has minor effect on the segregation (Fig.11.), high amount shows major effect (Fig.12.).

The real glass bead content can be described with the following (1) equation:

$$\Phi_v(\Phi_n; d; L) = \Phi_n \cdot [d \cdot (c_1 \cdot L + c_2) + 1], \quad (1)$$

where  $\Phi_v(\Phi_n; d; L)$  [%] is the local glass bead content,  $\Phi_n$  [%] is the nominal glass bead content (original content, before injection molding),  $d$  [ $\mu\text{m}$ ] is the average diameter of the glass beads,  $L$  [mm/mm] is the relative flow length and  $c_1$  and  $c_2$  are material and technology dependent constants. These constants are  $c_1 = 2.03 \cdot 10^{-3}$  [ $1/\mu\text{m}$ ] and  $c_2 = -1.07 \cdot 10^{-3}$  [ $1/\mu\text{m}$ ], using PA6 with glass beads. The equation was verified on a 2 mm thick, 80 mm by 80 mm plate with glass bead contents ranging 0-40 wt% and diameter ranging 11-203  $\mu\text{m}$ . For these boundary conditions the correlation ( $R^2$ ) between calculated and measured values was 0.995.

Based on the migration of the particles along the flow path the properties of the material could change along the flow direction. It can be assumed that the shrinkage properties will change in the flow direction as the local content of the particles diverges from its nominal value.

The longitudinal shrinkage, which is parallel to the flow direction, was measured at three locations (Fig.2.).  $L_0$ ,  $L_1$  and  $L_2$  were found to be the same. This is consistent with the segregation measurements; for the particular mold (runner and gate) design, the flow was apparently uniform and there were only minor differences between particle contents (Fig.5.). Although the longitudinal shrinkage is not necessarily uniform along the flow direction, the average value is apparently the same at different locations along the cross flow direction.

It is quite different in the cross-flow direction. Based on the segregation measurement it is expected that the shrinkage in cross-flow direction at the gate is different than that at the end of the flow.

This shrinkage difference will result from the pressure distribution and from the segregation. At the gating area, the shrinkage is on the one hand lower due to the pressure drop along the flow; in the other hand it is higher due to the particle content being lower in this area. Thus theoretically these two parameters have opposite effects on the local shrinkage.

Using the Moldflow Plastics Insight 6.2 (MPI 6.2) injection molding simulation software, it can be observed that the pressure is linearly decreasing along the flow path using PA6 without the fillers (Fig.13.).

As the pressure decreases the volumetric shrinkage increases (Fig.14.), meaning that the pressure induced shrinkage is lower in the gating zone than at the end of the flow.

Using filled materials the pressure drop increases due to an increase in viscosity. Based on this effect only, the shrinkage difference should be greater in filled materials. But in contradiction to this effect, segregation will also have an influence on the shrinkage the opposite way. As the pressure increases, the migration will be more significant and the growing volume fraction of the particles will decrease the shrinkage itself.

The cross-flow shrinkage was influenced by the glass bead content and its diameter as well as the flow length. It was concluded that the migration of the glass beads has a significant effect on the cross-flow shrinkage, which can be described by the following (2) equation:

$$S(L; \Phi_v; d) = L \cdot [\Phi_v \cdot (c_3 \cdot d + c_4) + m_0] + c_5 \cdot \Phi_v + S_0 \quad , \quad (2)$$

where  $S(L; \Phi_v; d)$  [%] is the local cross-flow directional shrinkage,  $L$  [mm] is the flow length,  $\Phi_v$  [%] is the local glass bead content,  $d$  [ $\mu\text{m}$ ] is the diameter of the beads,  $S_0$  is the cross-flow directional shrinkage of the unfilled material,  $m_0$  is the shrinkage change of the unfilled material as a function of the flow length, and  $c_3$ ,  $c_4$  and  $c_5$  are material and technology dependent constants. These constants are  $c_3 = -2.0 \cdot 10^{-7}$  [1/ $\text{mm}^2$ ],  $c_4 = -1.0 \cdot 10^{-5}$  [1/mm],  $c_5 = -8.9 \cdot 10^{-3}$  [-],  $S_0 = 1.19$  [%] and  $m_0 = 2.11 \cdot 10^{-3}$  [%/mm], using PA6 with glass beads. The equation was verified on a 2 mm thick, 80 mm by 80 mm plate with glass bead content ranging 0-40 wt% and diameter ranging 11-203  $\mu\text{m}$ . For these boundary conditions the correlation ( $R^2$ ) was 0.975.

It can be seen on the following figures (Fig.15-16.) that the shrinkage compensation with the migration effect using small beads eliminates a minor deviation only.

Using the smallest glass beads the deviation can be neglected (Fig.15.), while using larger (85  $\mu\text{m}$ ) beads the deviation is higher, but plays only a minor role in the shrinkage calculations (Fig.16.).

While these bead sizes (11 and 85  $\mu\text{m}$ ) have insignificant influence on the migration induced shrinkage, the two largest sizes (156 and 203  $\mu\text{m}$ ) have major influence on the migration induced shrinkage calculations (Fig.17-18.).

Although the large glass beads (156 and 203  $\mu\text{m}$ ) have a major effect on shrinkage, large deviation can only be detected with higher glass bead contents. As the glass bead content increases the deviation increases between the non-compensated and compensated model where the migration based particle content was taken into consideration for the shrinkage calculations.

To understand the difference between the compensated and non-compensated case the following (3) equation can be derived from (1) and (2):

$$S_{segr} = \Phi_n \cdot d \cdot \left[ L \cdot (c_3 \cdot d + c_4) \cdot (c_1 \cdot L + c_2) \right] + c_5 \cdot (c_1 \cdot L + c_2), \quad (3)$$

where  $S_{segr}$  [%] the segregation induced cross-flow directional shrinkage,  $\Phi_n$  [%] is the nominal glass bead content,  $d$  [ $\mu\text{m}$ ] is the diameter of the beads,  $L$  [mm] is the flow length, and  $c_1$ ,  $c_2$ ,  $c_3$ ,  $c_4$  and  $c_5$  are material and technology dependent constants.

Finally, it should be emphasized that the deviation caused by the segregation effect is highly dependant on the filler size and content. Using high content of the filler (40 wt%) the glass bead size plays a major role in the segregation induced shrinkage calculation (Fig.19.).

While the smallest filler (11  $\mu\text{m}$ ) has a negligible influence on segregation, the largest filler (203  $\mu\text{m}$ ) has significant influence (Fig.20.) that could be as high as 25% along the flow path.

A similar effect can be found by examining the largest glass beads with different contents (Fig.21.). The most important difference is that the lowest content of the fillers (10 wt%) has higher influence than the highest content for the smallest beads had.

Similarly for the filler sizes, while the smallest filler content (10 wt%) has insignificant influence on this effect, the highest content (40 wt%) has large influence (Fig.22.) similarly as previously (about 25% along the flow path).

## 6. Conclusion

A new method was introduced to evaluate the segregation effect of glass beads in 40 wt% glass beads filled material. It was concluded that independently from the flow length the gravity effect can be neglected.

It was concluded that the flow-directional segregation strongly depends on both the diameter and the concentration of the glass beads. In addition, segregation affects the distribution of volumetric shrinkage along the flow path, playing a major role on the dimensional accuracy of the part. Based on these measurements the local glass bead content was described with an equation. The cross-flow shrinkage varied along the flow length, and was influenced by both the glass bead content and the bead diameter. It was concluded that the migration of the glass beads has a significant effect on the cross-flow shrinkage, which can be also described with an equation.

Based on these two statements it was highlighted that a standard shrinkage calculation has an error which grows with increased particle migration. Using high

content of fillers the glass bead size plays a major role in the segregation induced shrinkage calculation, where the error of the calculation can be as high as 25 percent.

## 7. Acknowledgement

This paper was supported by the János Bolyai Research Scholarship of the Hungarian Academy of Sciences. The author would like to thank Arburg Hungaria Ltd. for the injection molding machine.

This work is connected to the scientific program of the "Development of quality-oriented and harmonized R+D+I strategy and functional model at BME" project. This project is supported by the New Hungary Development Plan (Project ID: TÁMOP-4.2.1/B-09/1/KMR-2010-0002).

## 8. References

- 1 S. Hashemi, *Express Polym. Lett.*, **2**, 474 (2008)
- 2 R.P. Hegler, and G. Mennig, *Polym. Eng. Sci.*, **25**, 395, (1985)
- 3 R.P. Hegler, G. Mennig, and C. Schmauch, *Adv. Polym. Tech.*, **7**, 3, (1987)
- 4 M.R. Kamal, and P. Singh, *ANTEC*, 240, (1989)
- 5 D. O'Regan, and M. Akay, *J. Mater. Process. Tech.*, **56**, 282, (1996)
- 6 E. Lafranche, P. Krawczak, J.P. Ciolczyk, and J. Maugey, *Adv. Polym. Tech.*, **24**, 114, (2005)
- 7 T.D. Papathanasiou, and S.O. Ogadhoh, *Scripta Metall Mater.*, **33**, 1133, (1995)
- 8 S.O. Ogadhoh, and T.D. Papathanasiou, *Compos. Part A-Appl S.*, **27**, 57, (1996)
- 9 S.C. Jana, *Polym. Eng. Sci.*, **43**, 570, (2003)
- 10 C.M. Hong, J. Kim, and S.C. Jana, *Polym. Eng. Sci.*, **44**, 2101, (2004)
- 11 C.M. Hong, and S.C. Jana, *ANTEC*, 1841, (2004)
- 12 E. Lafranche, P. Krawczak, J.P. Ciolczyk, and J. Maugey, *Express Polym. Lett.*, **1**, 456, (2007)
- 13 Y.C. Lam, X. Chen, K.C. Tam, and S.C.M. Yu, *J. Manuf. Sci. Eng.*, **125**, 538, (2003)

- 14 F. Gadala-Maria, *Acrivos J. Rheol.*, **24**, 799, (1980)
- 15 D. Leighton, and A. Acrivos, *J. Fluid Mech.*, **177**, 109, (1987)
- 16 D. Leighton, and A. Acrivos, *J. Fluid Mech. Digit. Arch.*, **181**, 415, (1987)
- 17 R.J. Phillips, R.C. Armstrong, R.A. Brown, A.L. Graham, and J.R. Abbott, *Phys. Fluids.*, **4**, 30, (1992)
- 18 M. Allende, and D.M. Kalyon, *J. Rheol.*, **44**, 79, (2000)
- 19 Y.C. Lam, X. Chen, K.W. Tan, M. Jan, K.C. Tam, and S.C.M. Yu, *J. Inj. Mold Tech.*, **6**, 45, (2002)
- 20 X. Chen, Y.C. Lam, K.W. Tan, J.C. Chai, and S.C.M. Yu, *Model. Simul. Mater. Sc.*, **11**, 503, (2003)
- 21 X. Chen, Y.C. Lam, Z.Y. Wang, and K.W. Tan, *Comp. Mater. Sci.*, **30**, 223, (2004)
- 22 Y.C. Lam, X. Chen, K.W. Tan, J.C. Chai, and S.C.M. Yu, *Compos. Sci. Technol.*, **64**, 1001, (2004)
- 23 G. Dogossy, and T. Czigány, *Polym. Advan. Technol.*, **17**, 825, (2006)
- 24 K. Prashantha, J. Soulestin, M.F. Lacrampe, E. Lafranche, P. Krawczak, G. Dupin, and M. Claes, *Express Polym. Lett.*, **3**, 630, (2009)

## 9. Figure captions

Figure 1. The injection mold used in the experiments

Figure 2. The measuring points for shrinkage determination (L0, L1 and L2 are the flow directional shrinkages measuring positions, while WG and WE are the measuring positions for the cross-flow directions' shrinkage close to the gate and at the end of the flow)

Figure 3. The nine measuring points for segregation

Figure 4. The 5 and 14 strips for the segregation measurements

Figure 5. The segregation of the glass beads at the nine measuring points, glass bead content is 40 wt%, the diameter of the glass beads is 203  $\mu\text{m}$

Figure 6. Flow directional measurements of the segregation, glass bead content is 40 wt%, the diameter of the glass beads is 203  $\mu\text{m}$

Figure 7. The segregation in the function of the glass bead content and flow length, in the case of 11  $\mu\text{m}$  diameter glass beads

Figure 8. The segregation in the function of the glass bead content and flow length, the diameter of the glass beads was 85  $\mu\text{m}$

Figure 9. The segregation in the function of the glass bead content and flow length, the diameter of the glass beads was 156  $\mu\text{m}$

Figure 10. The segregation in the function of the glass bead content and flow length, the diameter of the glass beads was 203  $\mu\text{m}$

Figure 11. The segregation in the function of the glass bead size and flow length, the nominal glass bead content was fixed to 10 wt%

Figure 12. The segregation in the function of the glass bead size and flow length, the nominal glass bead content was fixed to 40 wt%

Figure 13. The pressure drop – calculated with MPI 6.2 – in the flow direction (0 is next to the gate, 80 is the end of the flow)

Figure 14. The volumetric shrinkage – calculated with MPI 6.2 – in the flow direction (0 is next to the gate, 80 is the end of the flow)

Figure 15. Linear shrinkages in cross-flow direction, measured points and calculated with (comp.) and without (non comp.) the segregation effect, 11  $\mu\text{m}$  diameter glass beads

Figure 16. Linear shrinkages in the cross-flow direction, measured points and the calculated with (comp.) and without (non comp.) the segregation effect, the diameter of the glass beads was 85  $\mu\text{m}$

Figure 17. Linear shrinkages in the cross-flow direction, measured points and the calculated with (comp.) and without (non comp.) the segregation effect, the diameter of the glass beads was 156  $\mu\text{m}$

Figure 18. Linear shrinkages in the cross-flow direction, measured points and the calculated with (comp.) and without (non comp.) the segregation effect, the diameter of the glass beads was 203  $\mu\text{m}$

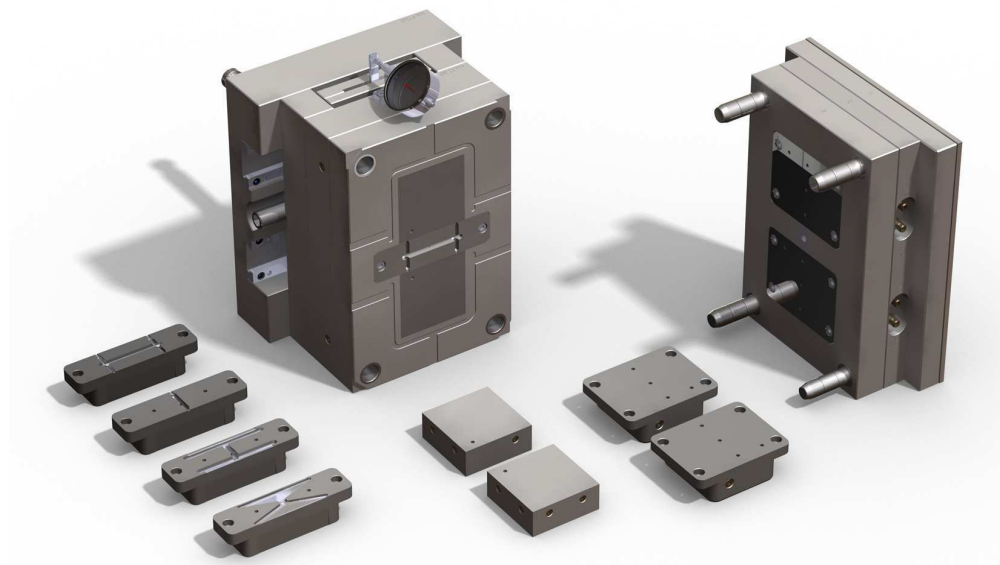
Figure 19. The segregation induced decrease of the shrinkage in the function of the flow length and the diameter of the glass beads, the nominal glass bead content was fixed to 40 wt%

Figure 20. Segregation induced percentage deviation of the shrinkage in the function of the flow length and the diameter of the glass beads, the nominal glass bead content was fixed to 40 wt%

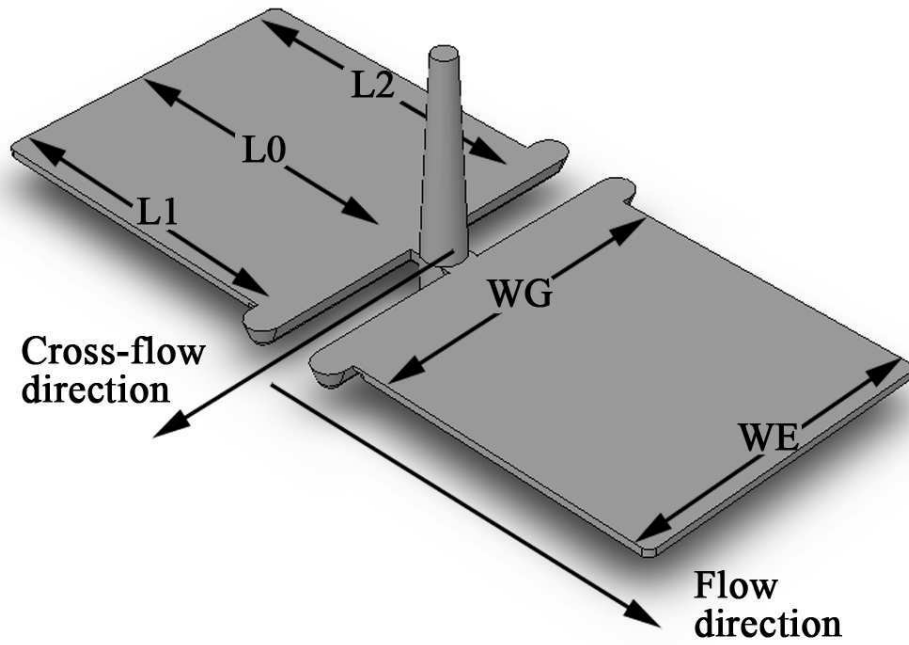
Figure 21. The segregation induced decrease of the shrinkage in the function of the flow length and the content of the glass beads, the diameter of the glass beads was 203  $\mu\text{m}$

Figure 22. Segregation induced percentage deviation of the shrinkage in the function of the flow length and the content of the glass beads, the diameter of the glass beads was 203  $\mu\text{m}$

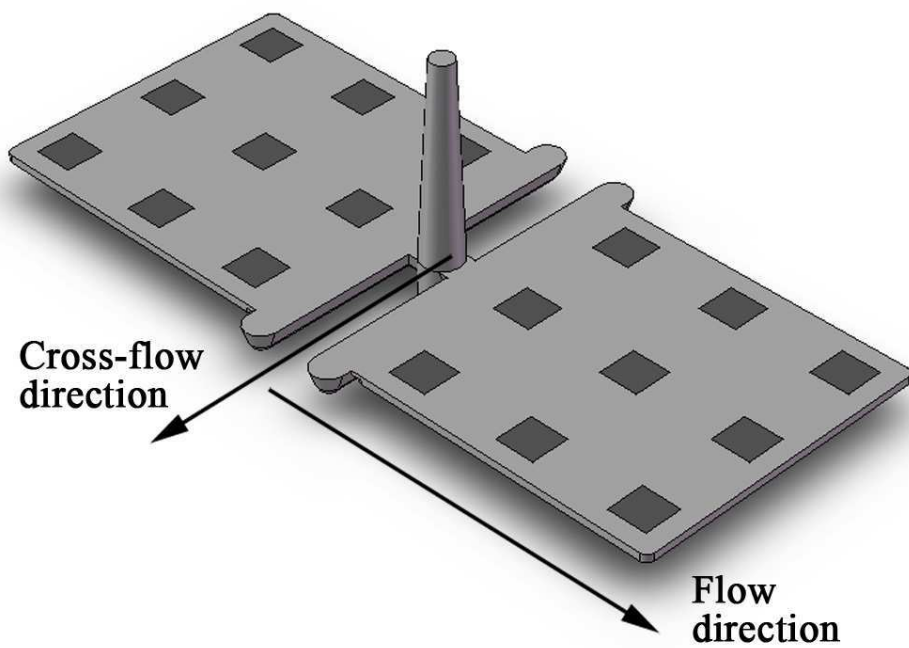
For Peer Review



The injection mold used in the experiments  
140x80mm (300 x 300 DPI)

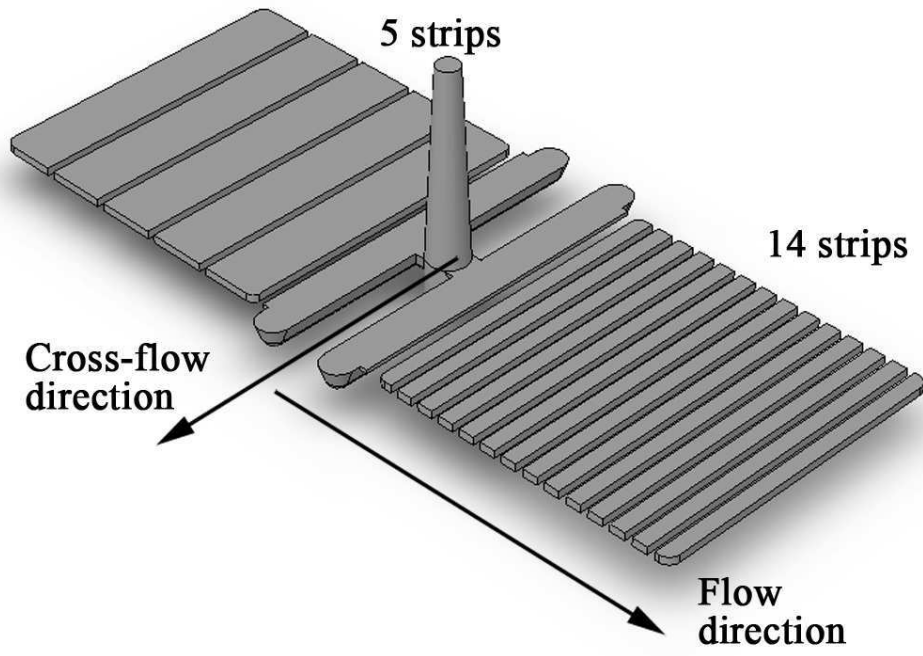


The measuring points for shrinkage determination (L0, L1 and L2 are the flow directional shrinkages measuring positions, while WG and WE are the measuring positions for the cross-flow directions' shrinkage close to the gate and at the end of the flow)  
90x60mm (300 x 300 DPI)



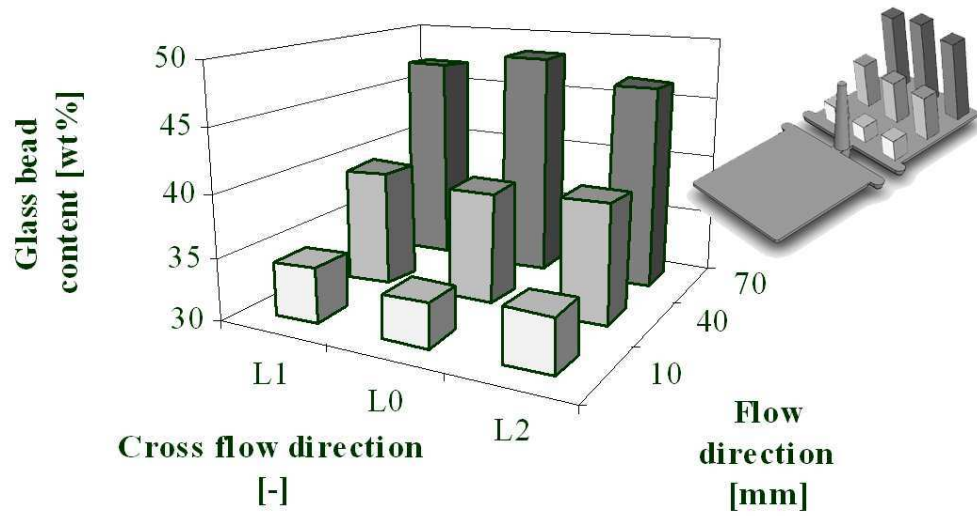
The nine measuring points for segregation  
90x60mm (300 x 300 DPI)

Review

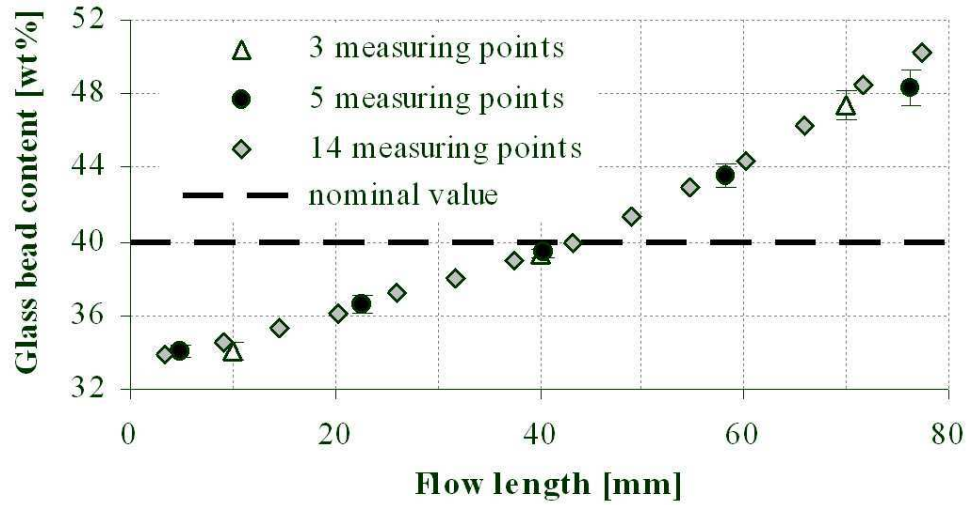


The 5 and 14 strips for the segregation measurements  
90x60mm (300 x 300 DPI)

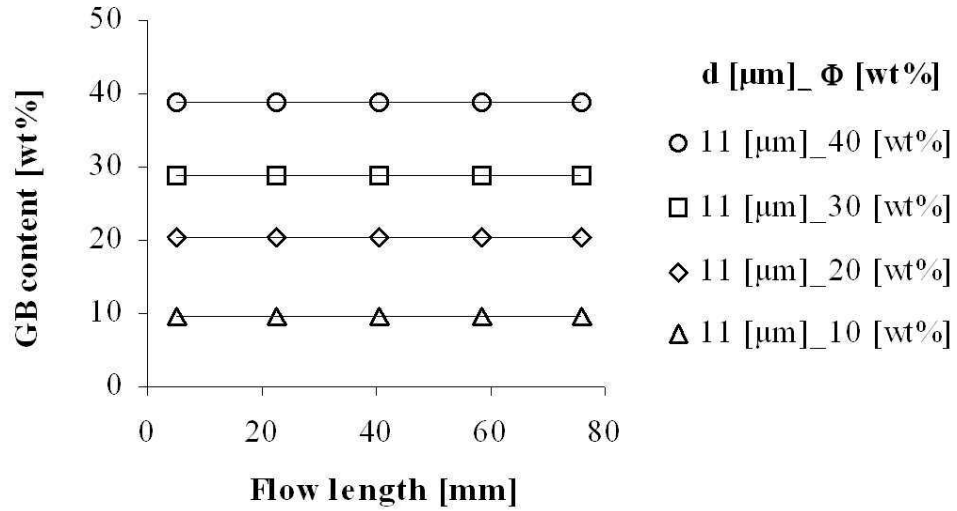
Review



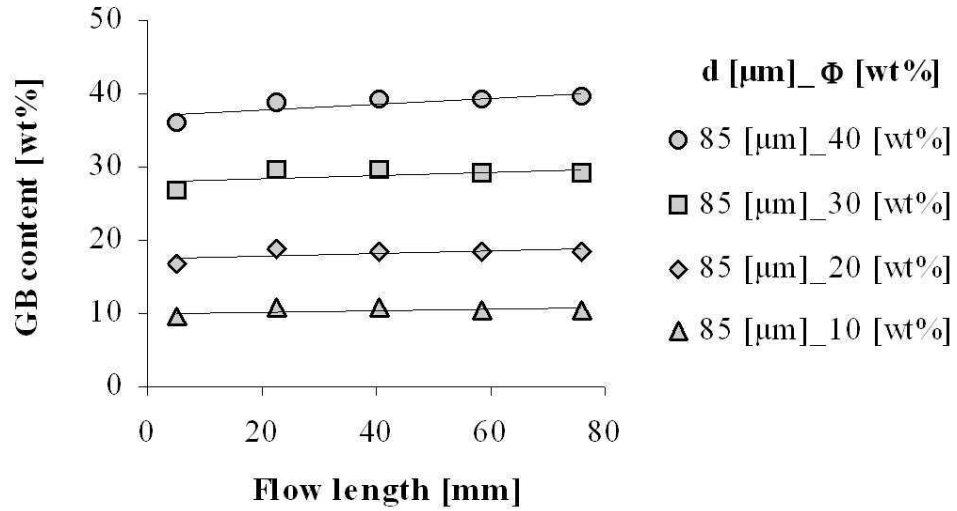
The segregation of the glass beads at the nine measuring points, glass bead content is 40 wt%, the diameter of the glass beads is 203  $\mu\text{m}$   
 90x50mm (300 x 300 DPI)



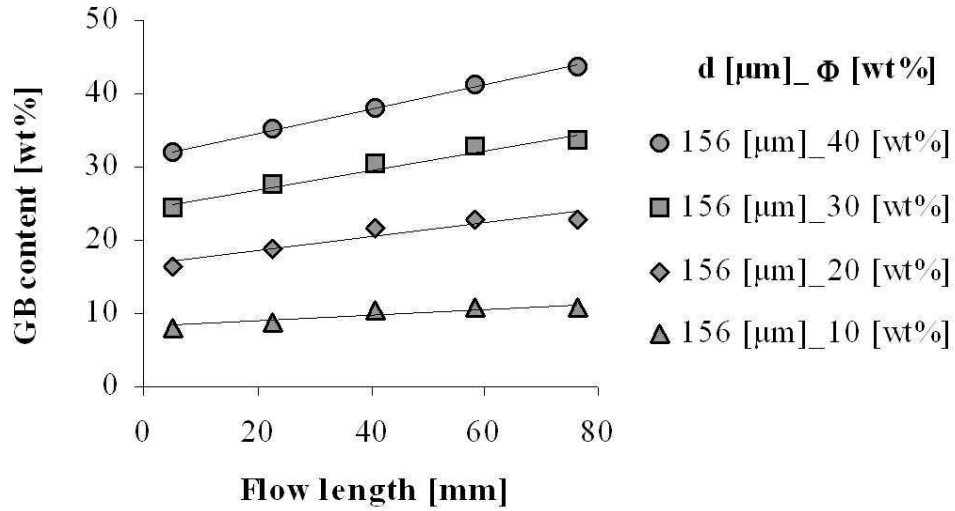
Flow directional measurements of the segregation, glass bead content is 40 wt%, the diameter of the glass beads is 203  $\mu\text{m}$   
90x50mm (300 x 300 DPI)



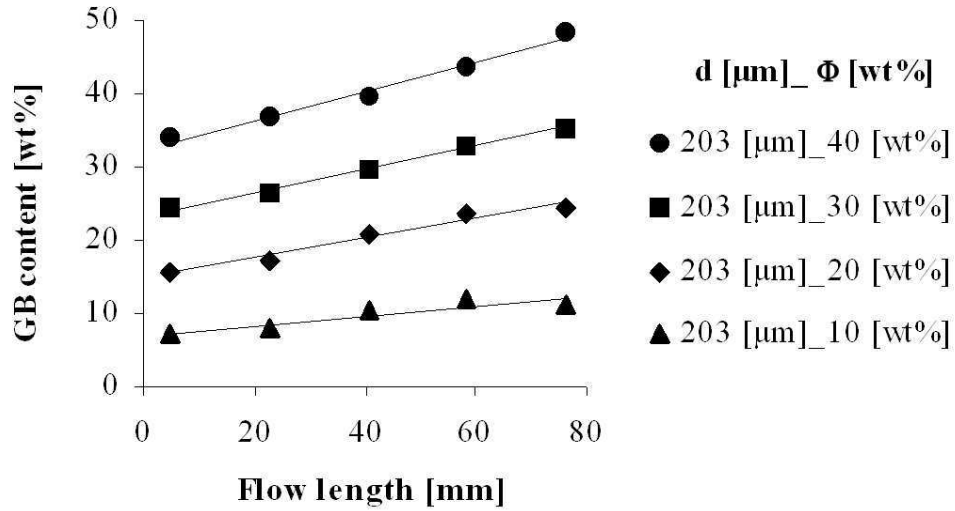
The segregation in the function of the glass bead content and flow length, in the case of 11 μm diameter glass beads  
90x50mm (300 x 300 DPI)



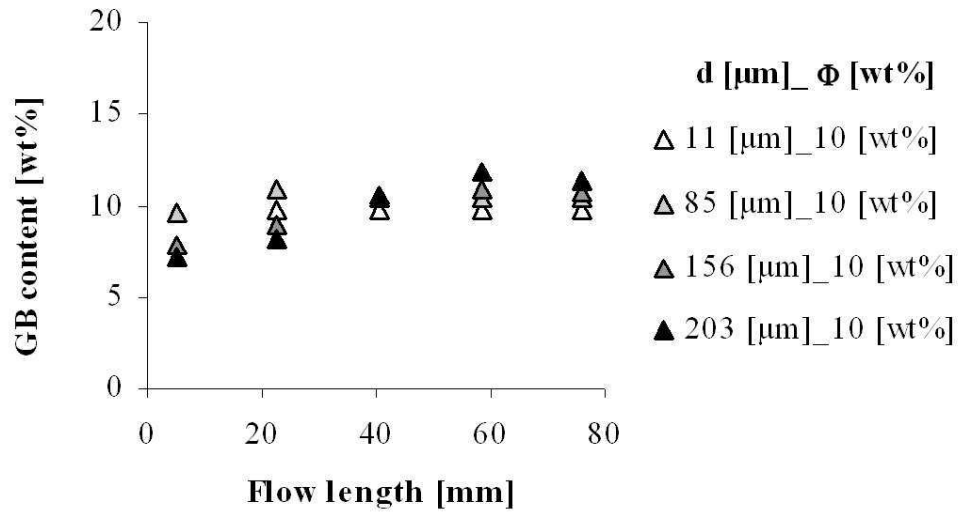
The segregation in the function of the glass bead content and flow length, the diameter of the glass beads was 85 μm  
90x50mm (300 x 300 DPI)



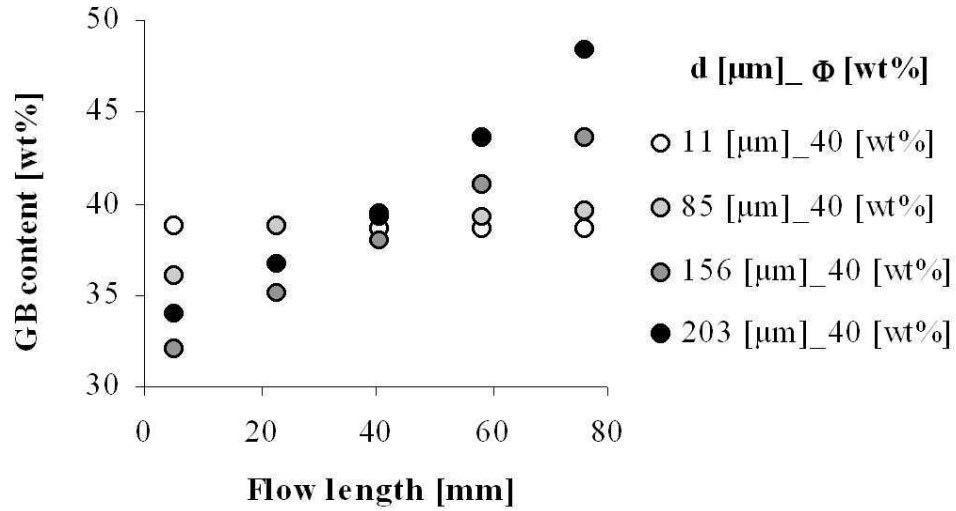
The segregation in the function of the glass bead content and flow length, the diameter of the glass beads was 156 μm  
90x50mm (300 x 300 DPI)



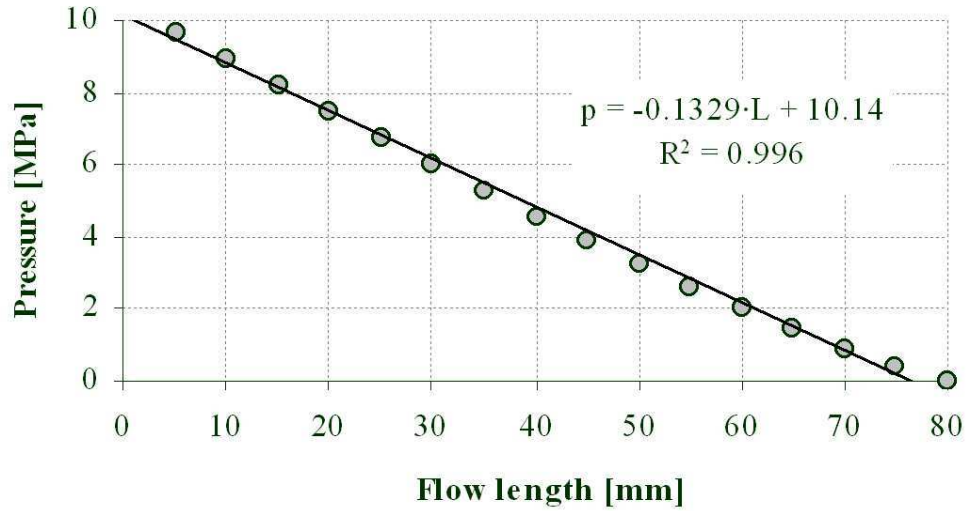
The segregation in the function of the glass bead content and flow length, the diameter of the glass beads was 203  $\mu\text{m}$   
90x50mm (300 x 300 DPI)



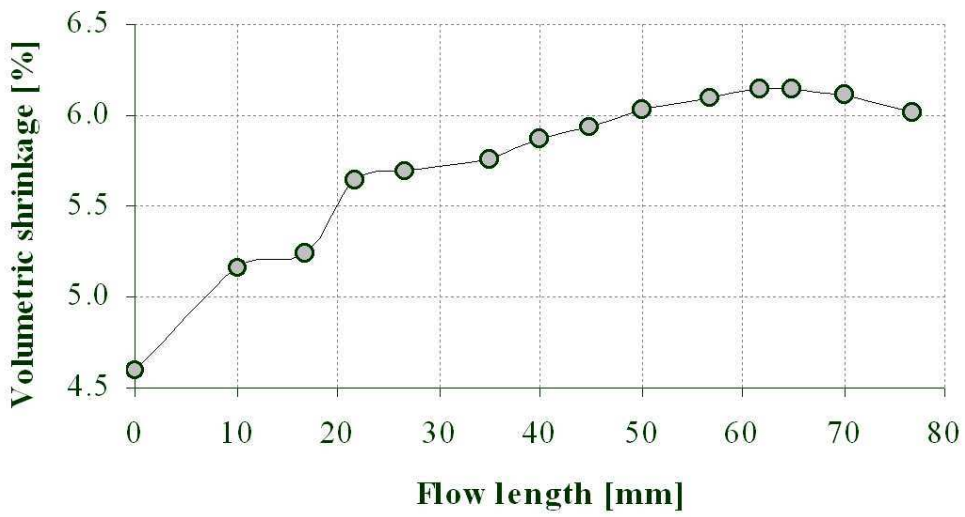
The segregation in the function of the glass bead size and flow length, the nominal glass bead content was fixed to 10 wt%  
 90x50mm (300 x 300 DPI)



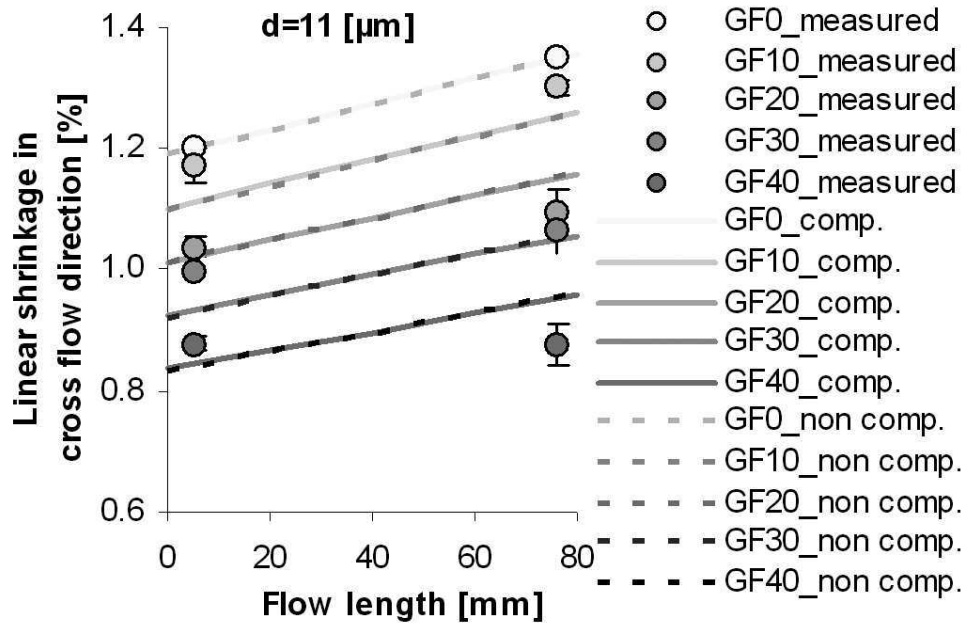
The segregation in the function of the glass bead size and flow length, the nominal glass bead content was fixed to 40 wt%  
90x50mm (300 x 300 DPI)



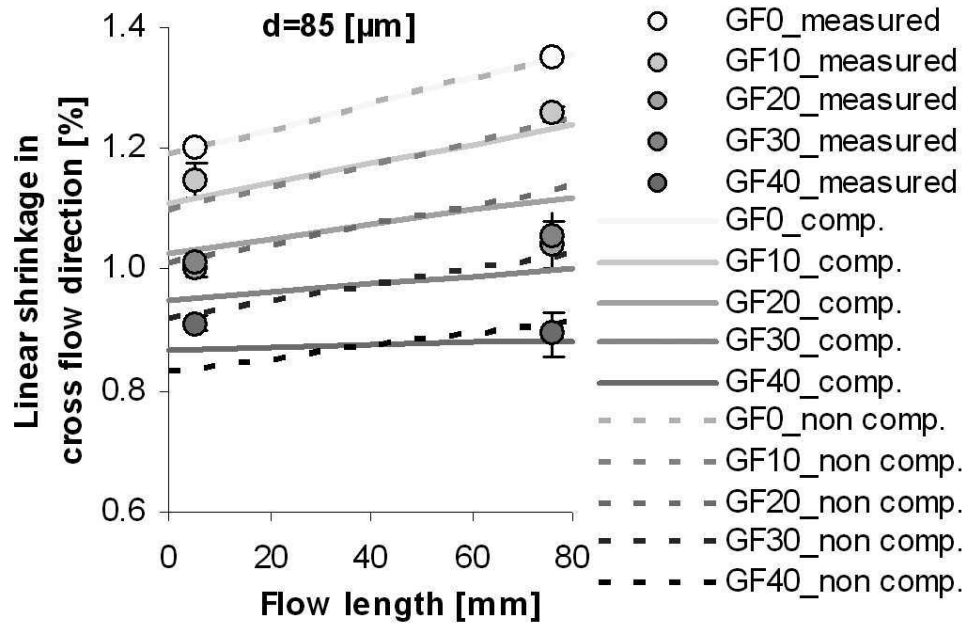
The pressure drop – calculated with MPI 6.2 – in the flow direction (0 is next to the gate, 80 is the end of the flow)  
 90x50mm (300 x 300 DPI)



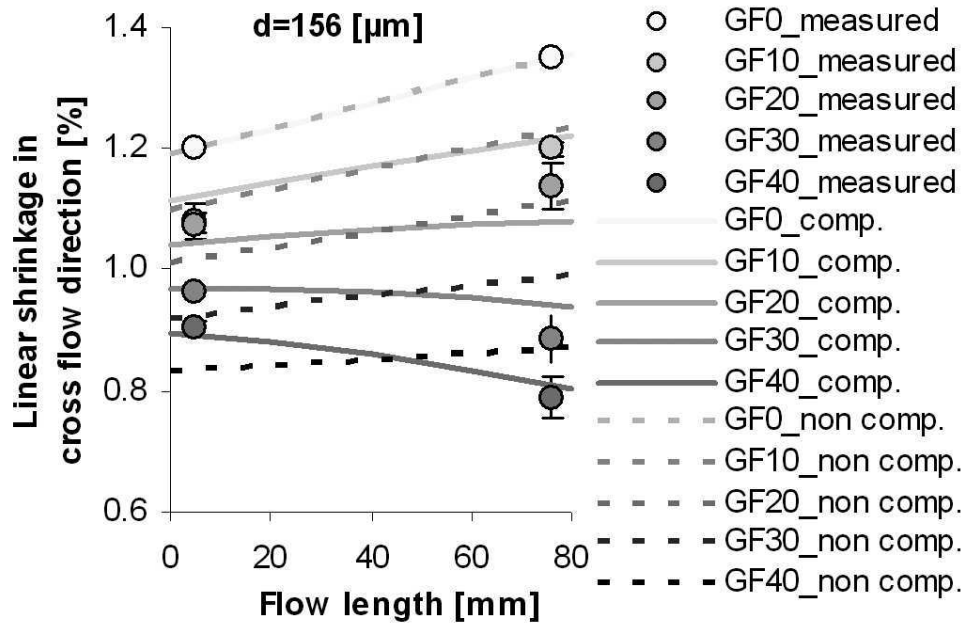
The volumetric shrinkage – calculated with MPI 6.2 – in the flow direction (0 is next to the gate, 80 is the end of the flow)  
90x50mm (300 x 300 DPI)



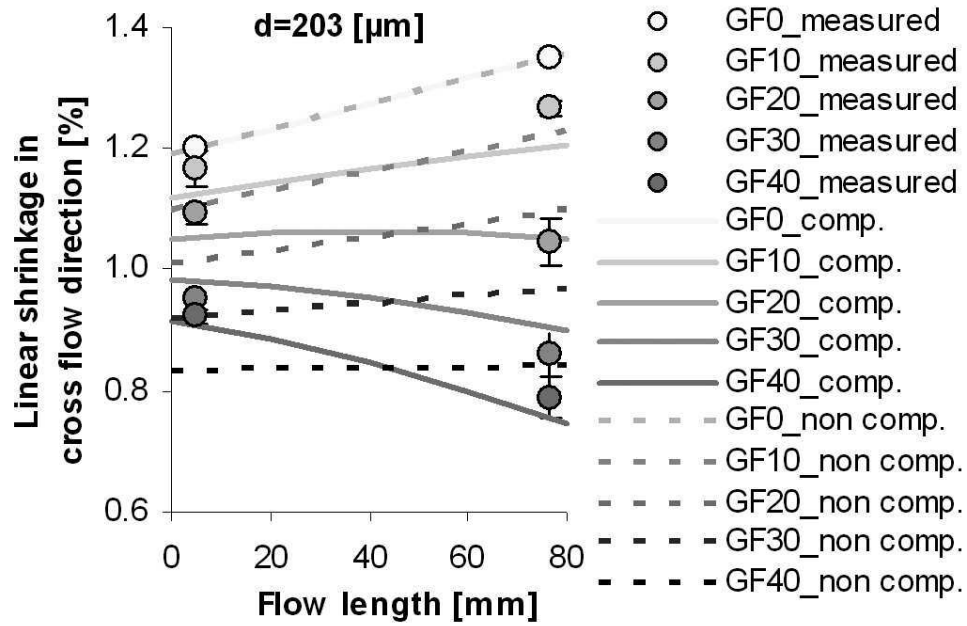
Linear shrinkages in cross-flow direction, measured points and calculated with (comp.) and without (non comp.) the segregation effect, 11 μm diameter glass beads  
90x60mm (300 x 300 DPI)



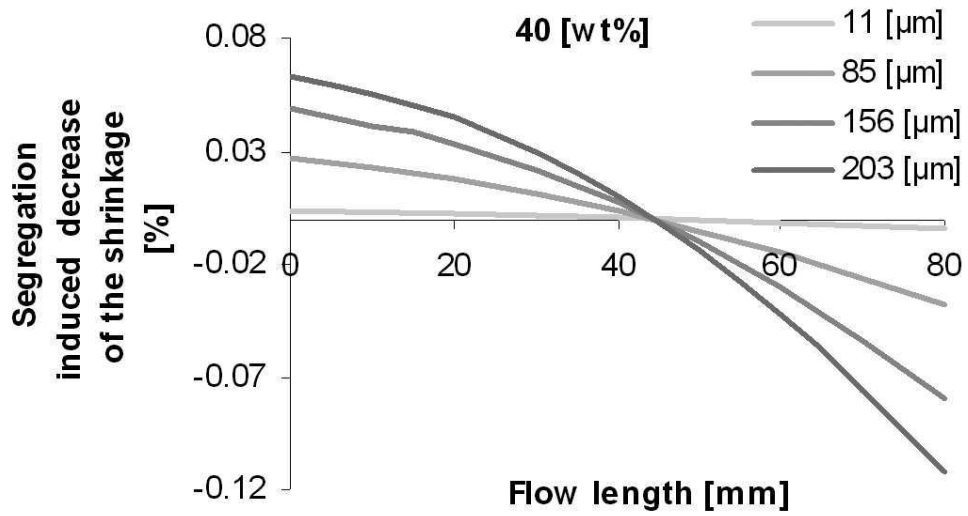
Linear shrinkages in the cross-flow direction, measured points and the calculated with (comp.) and without (non comp.) the segregation effect, the diameter of the glass beads was 85 μm 90x60mm (300 x 300 DPI)



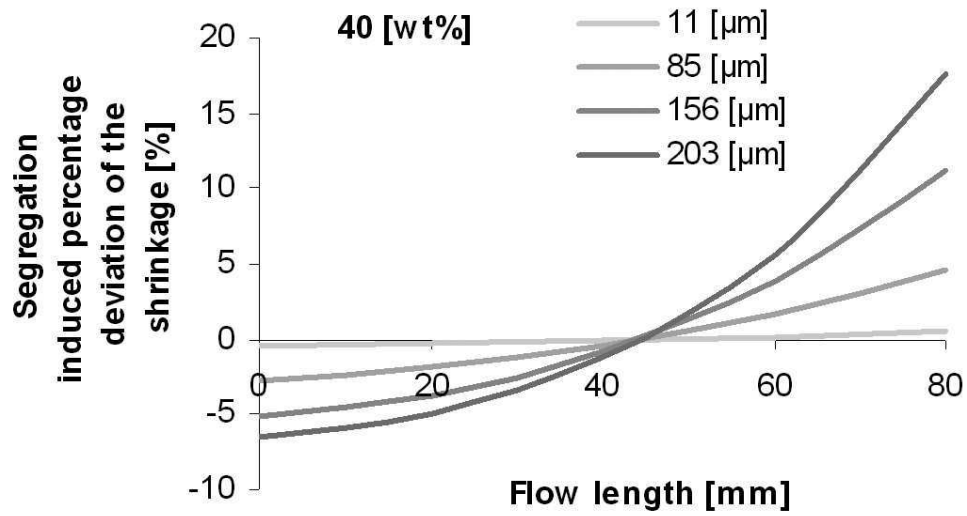
Linear shrinkages in the cross-flow direction, measured points and the calculated with (comp.) and without (non comp.) the segregation effect, the diameter of the glass beads was 156 μm 90x60mm (300 x 300 DPI)



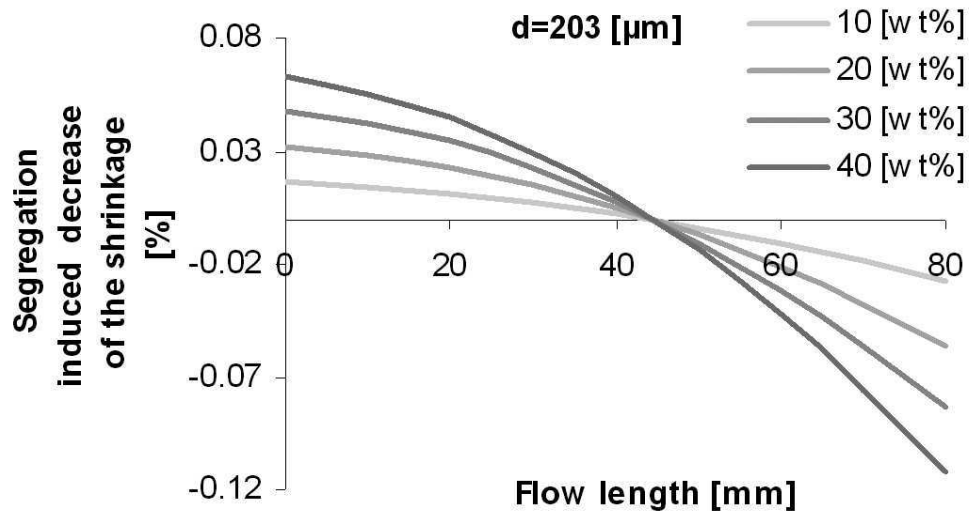
Linear shrinkages in the cross-flow direction, measured points and the calculated with (comp.) and without (non comp.) the segregation effect, the diameter of the glass beads was 203  $\mu\text{m}$   
90x60mm (300 x 300 DPI)



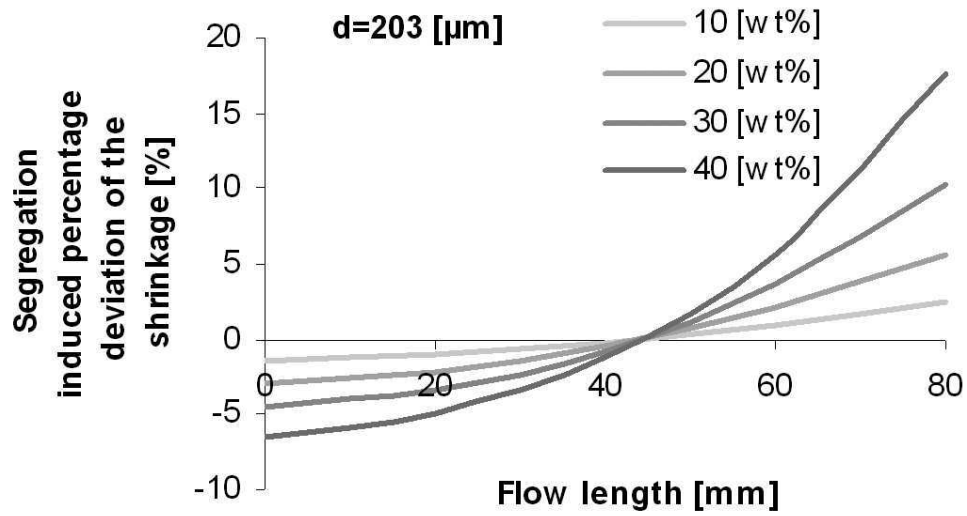
The segregation induced decrease of the shrinkage in the function of the flow length and the diameter of the glass beads, the nominal glass bead content was fixed to 40 wt%  
90x50mm (300 x 300 DPI)



Segregation induced percentage deviation of the shrinkage in the function of the flow length and the diameter of the glass beads, the nominal glass bead content was fixed to 40 wt%  
90x50mm (300 x 300 DPI)



The segregation induced decrease of the shrinkage in the function of the flow length and the content of the glass beads, the diameter of the glass beads was 203 μm  
90x50mm (300 x 300 DPI)



Segregation induced percentage deviation of the shrinkage in the function of the flow length and the content of the glass beads, the diameter of the glass beads was 203 µm  
90x50mm (300 x 300 DPI)